Aerosol Science and Technology
Publication details, including instructions for authors and subscription information:
http://www.tandfonline.com/loi/uast20

Modal Aerosol Dynamics Modeling

Evan R. Whitby [a] & Peter H. McMurry [b]

[a] CHIMERA TECHNOLOGIES, INC., 15051 ZODIAC ST. NE, (E.R.W.), FOREST LAKE, MINNESOTA, 55025

[b] MECHANICAL ENGINEERING DEPARTMENT, UNIVERSITY OF MINNESOTA, 111 CHURCH ST. SE, (P.H.MCM), MINNEAPOLIS, MINNESOTA, 55455

Version of record first published: 13 Jun 2007.

To cite this article: Evan R. Whitby & Peter H. McMurry (1997): Modal Aerosol Dynamics Modeling, Aerosol Science and Technology, 27:6, 673-688

To link to this article: http://dx.doi.org/10.1080/02786829708965504

Modal Aerosol Dynamics Modeling

Evan R. Whitby and Peter H. McMurry*
CHIMERA TECHNOLOGIES, INC.,
15051 ZODIAC ST. NE,
FOREST LAKE, MINNESOTA 55025 (E.R.W.)
AND MECHANICAL ENGINEERING DEPARTMENT,
111 CHURCH ST. SE,
UNIVERSITY OF MINNESOTA,
MINNEAPOLIS, MINNESOTA 55455 (P.H.MCM)

ABSTRACT. The derivation of the governing equations for modal aerosol dynamics (MAD) models is presented. MAD models represent the aerosol size distribution as an assemblage of distinct populations of aerosol, where each population is distinguished by size or chemical composition. The size distribution of each population is approximated by an analytical modal distribution function; usually by a lognormal distribution function. By substituting the MAD representation of aerosol size distributions into the governing equation for aerosol processes, the governing differential equations for MAD models are derived. These differential equations express the time dependence of the moments of the aerosol size distribution and are called Moment Dynamics Equations (MDEs). The MDEs for Continuously-Stirred Tank Aerosol Reactors (CSTARs) are also derived. AEROSOL SCIENCE AND TECHNOLOGY 27:673–688 (1997) © 1997 American Association for Aerosol Research

INTRODUCTION

Numerical models can be viewed as mathematical frameworks that permit the interaction of complex physical processes to be simulated. For processes in the atmosphere, computer simulations are indispensable for extending the understanding gained through experimental measurements, permitting the environmental impact of anthropogenic and biogenic sources of gases, vapors, and particles to be assessed. In chemical reactors it is often difficult to measure aerosol size distributions because the gases may be either toxic, corrosive, or explosive, or the systems may be operated at low pressures (most aerosol measurement systems operate at near atmospheric pressure). In these cases mathematical modeling of aerosol processes is useful for extending the knowledge gained by an otherwise limited set of experimental data.

The first step in developing a numerical aerosol model is to assemble expressions for the relevant physical processes, such as chemical reactions, nucleation, condensation, coagulation, etc. The next step is to approximate the particle size distribution with a mathematical size distribution function. An aerosol model that can treat nucleation of vapors to form particles, must represent the size distribution of clusters (monomer, dimers, trimers, etc.) as well as particles. The size distribution of clusters is

*Correspondence to: Evan Whitby, Chimera Technologies, Inc., 15051 Zodiac St. NE, Forest Lake, Minnesota 55025. e-mail:Evan@ChimeraTech.com

Aerosol Science and Technology 27:673–688 (1997)

Published by Elsevier Science Inc.

0278-6826/97/$17.00
PII S0278-6826(97)00109-8

represented as the number concentration of each discrete cluster size, whereas the size distribution of particles is represented with a continuous distribution function.

The representation of the particle size distribution is so important in aerosol dynamics modeling, that most aerosol simulation techniques are categorized by the mathematical representation of the particle size distribution as discrete, spline, sectional, modal, or monodisperse (see Fig. 1). Note that although the Discrete/Spline and Discrete/Modal representations appear similar, the spline curve is a single continuous function, whereas the modal curve is the superposition of multiple, distinct distribution functions. A detailed review of available modeling techniques is provided by Whitby et al. (1991) and by Williams and Loyalka (1991), and the strengths, limitations, and key references of each model type is summarized in Table 1.

The modal technique represents the aerosol as multiple, independent populations of aerosol, called modes. The aerosol within each mode is represented by a separate mode size distribution function, and the output from modal models is the set of parameters for all modal size distributions. The number of modes is usually limited to two or three, so the accuracy is strongly influenced by the degree to which the modal size distribution functions represent the size distribution of the actual aerosol.

We refer to the mathematical modeling technique built around the modal representation of the aerosol size distribution as *modal aerosol dynamics* (MAD) modeling. Despite the extensive use of MAD models, no derivation or comprehensive description of the general modeling approach exists in the open literature. We therefore present a detailed description of the modal aerosol dynamics model and a derivation of the governing differential equations, called Moment Dynamics Equations (MDEs). We also show the derivation of the MDEs for simulating aerosol dynamics in Continuously-Stirred Tank Aerosol Reactors (CSTARs). A comparison of simulated (using the MAD model) and measured aerosol formation, transport, and deposition inside chemical reactors is given by Whitby and Hoshino (1996).

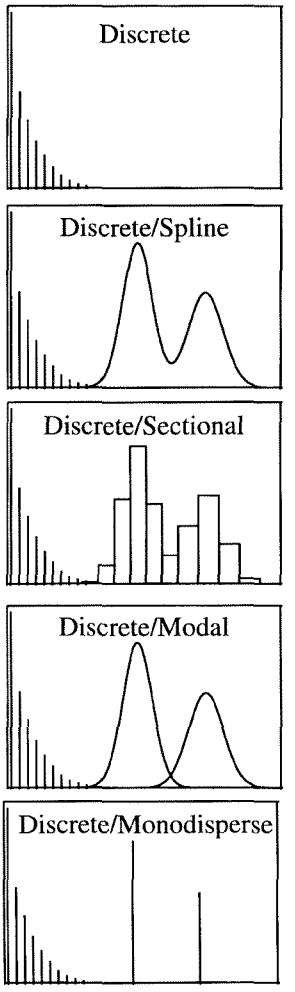

FIGURE 1. Representations of cluster and particle size distributions. Use of the discrete representation with the particle distribution functions is optional.

BASIC FEATURES OF AEROSOL MODELS

The goal of aerosol modeling is to determine the aerosol size distribution function for every point of interest in time and space.

TABLE 1. Comparison of Available Numerical Aerosol Modeling Techniques

Model Type	Strengths	Limitations	Key References
Spline	Accurate	Nonphysical distribution functions possible, computationally intensive	Middleton and Brock (1976); Gelbard and Seinfeld (1978)
Sectional	Flexible model structure multicomponent simulations, well developed codes and user interfaces available	Significant numerical diffusion for particle growth, computationally intensive, accuracy dependent on number of sections used to discretize size distribution	Gelbard and Seinfeld (1980)
Modal	Flexible model structure and computationally fast	Accuracy dependent on the form of the mode distribution functions	Whitby et al. (1991) and this work
Moment	Computationally very fast and accurate tracking of integral moments	Only available for a limited set of processes for which a closed set of moment equations can be derived	Friedlander (1983)
Monodisperse	Flexible model structure and computationally very fast	Only useful for rough estimate of aerosol dynamics, no size-distribution information	

This is accomplished by selecting a mathematical representation for the size distribution and expressing the effect of the aerosol processes on this mathematical function. In the following sections we review the physical processes affecting aerosol behavior, and the differential equations used to express the effect of these processes on the aerosol size distribution.

Aerosol Processes

The processes affecting aerosol behavior are represented pictorially in Fig. 2. The processes are depicted as acting within or at/across a control-volume boundary. Processes that act within the system boundaries are often called *internal processes*, and processes that act at/across system boundaries are often called *external processes* (Friedlander, 1977). The control volume can represent an entire system whose contents are homogeneously distributed throughout the control volume, or one control volume from a larger calculation domain. The processes depicted in Fig. 2 can be classified as shown in Table 2.

Diffusion across a boundary layer near the wall of a closed vessel is treated as a wall loss term and the deposition velocity, ν_d, is represented as

$$\nu_d = D/\delta_{bl}, \tag{1}$$

where D is the particle diffusion coefficient, and δ_{bl} is the boundary-layer thickness.

Differential Equations for the Parameters of n

In MAD models, we usually represent the aerosol size distribution with three-parameter distribution functions that can be classified by the total number concentration, N, an average size, $\bar{d}$, and a variance parameter, σ. For simulations that only involve internal processes (e.g., coagulation and volume growth), it is sometimes possible to directly obtain solutions to the differential equations for N, $\bar{d}$, and σ [see, for exam-

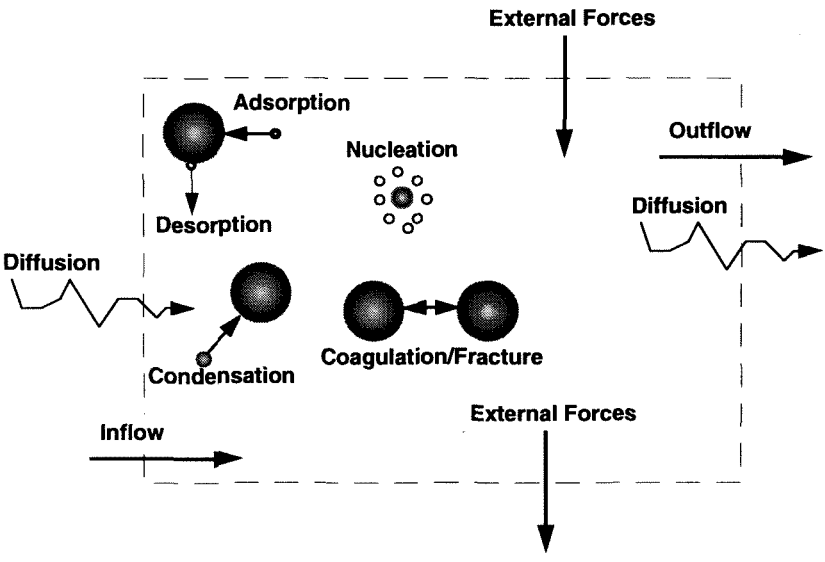

(a)

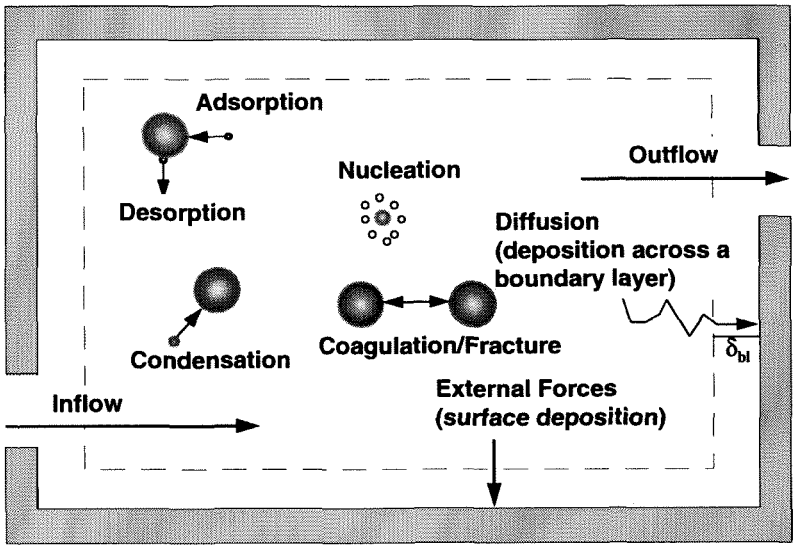

(b)

FIGURE 2. Aerosol dynamics processes for a control volume. (a) open system without walls; (b) open system with walls.

ple, Lee (1983) and Lee et al. (1990)]. A problem occurs, however, if the model is generalized to account for internal and external processes. For example, for combined coagulation and diffusion the differential equation for N (an integral moment) is

$$\frac{\partial}{\partial t}(N) = \frac{\partial}{\partial t}(N)_{\text{coag}} + \frac{\partial}{\partial t}(N)_{\text{diff}}. \qquad (2)$$

TABLE 2. Processes Affecting Aerosols

Internal Processes	External Processes
Coagulation	Diffusion
Fragmentation	Convection
Particle growth	Particle migration due to external forces
condensation/evaporation of vapors	deposition to surfaces in a closed system
adsorption/desorption of gases,	convection-like fluxes in an open system
absorption of gases	
reactions on or within particles	
Internal sources/nucleation	
fracture of bulk-phase material	
reentrainment of particles from surfaces	

Analogous equations for intensive parameters such as $\bar{d}$ and σ are not easily obtained. In other words, we can count the total number of particles crossing a boundary, but we cannot count anything like the average diameter or the width of the distribution crossing a boundary; these concepts have no meaning. We can avoid this problem by replacing the differential equations for $\bar{d}$ and σ with differential equations for two integral moments, which are extensive parameters. The resulting set of differential equations for each mode are called moment dynamic equations and are written as

$$\frac{\partial}{\partial t}(M_k) = f(N, \bar{d}, \sigma, T, P, \ldots), \tag{3}$$

where $M_k = \int_0^\infty d_p^k n(d_p) \mathrm{d}d_p$. Note that in this nomenclature $N = M_0$.

The effect of the processes affecting aerosol behavior can therefore be simulated by solving for the temporal and spatial evolution of independent moments of n, equal in number to the number of independent parameters of the mathematical function used to approximate n. To recover the distribution parameters, we need conversion equations to calculate $\bar{d}$ and σ in terms of M_k. Because lognormal distribution functions are commonly used in MAD models, we show the relationships between $\bar{d}$, σ, and M_k for lognormal distributions in Appendix A.

Equation (3) represents the system of equations that are solved in MAD models. In the following sections we derive the form of the differential equations used in Eq. (3).

General Dynamics Equation for Aerosols

The mathematical expression of the effect of the processes depicted in Fig. 2 on the aerosol size distribution is referred to as the *general dynamic equation* (GDE) for aerosols. The GDE has the following form (Friedlander [1977]):

$$\begin{aligned}\frac{\partial}{\partial t} n(v_p) = &\underbrace{-\nabla\cdot \mathbf{v} n(v_p)}_{\text{convection}} \underbrace{-\nabla\cdot \mathbf{c}(v_p) n(v_p)}_{\text{external forces}} + \underbrace{\nabla\cdot D(v_p)\nabla n(v_p)}_{\text{diffusion}} \\ &+ \underbrace{\frac{1}{2}\int_0^{v_p} \beta(\tilde{v}_p, v_p - \tilde{v}_p) n(\tilde{v}_p) n(v_p - \tilde{v}_p)\mathrm{d}\tilde{v}_p - \int_0^\infty \beta(\tilde{v}_p, \tilde{v}_p) n(v_p) n(\tilde{v}_p)\mathrm{d}\tilde{v}_p}_{\text{coagulation}} \\ &+ \underbrace{\left[\frac{\partial}{\partial t} n(v_p)\right]_g}_{\text{particle growth}} + \underbrace{\dot{n}_s(v_p)}_{\text{internal sources}},\end{aligned} \tag{4}$$

where n is the arbitrary size distribution function. For situations where detailed knowledge of the distribution function is unimportant, an expression similar to Eq. (4) can be written for the time rate of change of integral moments, M_k, of the distribution as [the derivation of the terms of Eq. (5) are given in Section 3]

$$\frac{\partial}{\partial t}(M_k) = \underbrace{\nabla\cdot\mathbf{v}M_k}_{\text{convection}} - \underbrace{\nabla\cdot\int_0^\infty d_p^k \mathbf{c}(d_p)n(d_p)\mathrm{d}d_p}_{\text{external forces}} + \underbrace{\nabla\cdot\int_0^\infty d_p^k D(d_p)\nabla n(d_p)\mathrm{d}d_p}_{\text{diffusion}}$$
$$+ \underbrace{\frac{1}{2}\int_0^\infty\int_0^\infty \left(d_{p_1}^3 + d_{p_2}^3\right)^{k/3}\beta(d_{p_1}, d_{p_2})n(d_{p_1})n(d_{p_2})\mathrm{d}d_{p_1}\,\mathrm{d}d_{p_2} - \frac{1}{2}\int_0^\infty\int_0^\infty \left(d_{p_1}^k + d_{p_2}^k\right)\beta(d_{p_1}, d_{p_2})n(d_{p_1})n(d_{p_2})\mathrm{d}d_{p_1}\,\mathrm{d}d_{p_2}}_{\text{coagulation}}$$
$$+ \underbrace{\int_0^\infty \frac{\mathrm{d}d_p^k}{\mathrm{d}v_p}\frac{\partial}{\partial t}(v_p)n(d_p)\mathrm{d}d_p}_{\text{particle growth}} + \underbrace{\int_0^\infty d_p^k \dot{n}_S(d_p)\mathrm{d}d_p}_{\text{internal sources}}. \tag{5}$$

We refer to Eq. (5) as the moment dynamic equation (MDE). For special forms of the rate coefficients, the integrals of Eq. (5) can be expressed in terms of other moments of the distribution without explicitly evaluating the integral terms. This results in expressions for the time rate of change of moments M_k in terms of other moments of the distribution. For some processes, a closed set of moment equations can be written and solved, and the resulting technique is referred to as the method of moments. Examples of the method of moments are given by Friedlander (1983), Kodas et al. (1986), Pratsinis et al. (1986), and others.

Although it is often possible to express the integrals of Eq. (5) directly in terms of other moments, it is not always possible to obtain closure of the resulting moment equations. A method that guarantees closure of the moment dynamic equations is to specify a mathematical form for the aerosol size distribution function, n. In the following sections, we describe the use of Eq. (5) when n is represented by one or more independent distribution functions.

The Modal Assumption. The preceding discussion assumes that a mathematical function is selected to represent n, but does not specify anything about n. Unlike aerosol models based on spline and sectional representations of n (e.g., see Middleton and Brock, 1976; Gelbard and Seinfeld, 1978; and Gelbard and Seinfeld, 1980), however, the selection of the mathematical representation of n in MAD models is motivated by the observed nature of many aerosol distributions. Specifically, experimental observations of atmospheric aerosols (e.g., see Whitby, 1978) indicate that many aerosol size distributions are composed of multiple aerosol populations, each originating from a distinct source. Based on this observation, the central physical assumption[1] of MAD

[1]Other physical assumptions and mathematical approximations are usually imposed when modeling a specific system, but these reflect choices made by the modeler rather than fundamental limitations of MAD models.

models is stated as follows:

An aerosol may be viewed as an assemblage of distinct populations of particles, distinguished by size or chemical composition. The size distribution of each population is approximated by an analytical distribution function.

Each distinct population is called a mode, giving rise to the name *modal aerosol dynamics* model. This assumption is hereafter referred to as the modal assumption. In a general case, a mode is required for each population of particles of a distinct size and/or chemical composition. As an aerosol ages, however, modes combine, so that the original structure becomes blurred or lost, and we ultimately represent an aged aerosol with fewer modes than the total number of distinct aerosol sources. The number of modes chosen, therefore, depends on the specific system and also on the modeler's interpretation of the processes affecting the system. The increased computational effort of using more modes may also influence a modeler's decision about how to represent an aerosol size distribution.

For a multimodal distribution, the overall distribution function is

$$n = \sum_{i=1}^{n_m} n_i, \tag{6}$$

where n_m is the number of aerosol modes. The MDE for a generalized multimodal distribution is obtained by substituting Eq. (6) into Eq. (5).

Because coagulation represents the interaction of multiple particles, substituting Eq. (6) into Eq. (5) and restricting the following discussion to two-body collisions, for coagulation of an aerosol with a bimodal distribution, we have *i-i*, intramodal coagulation, *i-j*, intermodal coagulation, and *j-j*, intramodal coagulation. We show the MDE for a bimodal distribution, and note that the intermodal coagulation terms for a distribution of three or more modes is a simple extension of the MDE for a bimodal distribution (considering the interactions between all pairs of modes). Substituting $n = n_i + n_j$ into Eq. (5) and separating terms yields the MDE for a bimodal aerosol (the separation of terms for coagulation is described in detail in Section 3.1.1).

MDE for Mode i

$$\begin{aligned}\frac{\partial}{\partial t}(M_{k_i}) = {} & \nabla\cdot\mathbf{v}M_{k_i} - \nabla\cdot\int_0^\infty d_p^k \mathbf{c}(d_p)n_i(d_p)\mathrm{d}d_p + \nabla\cdot\int_0^\infty d_p^k D(d_p)\nabla n_i(d_p)\mathrm{d}d_p \\ & + \frac{1}{2}\int_0^\infty\int_0^\infty \left(d_{p_1}^3 + d_{p_2}^3\right)^{k/3}\beta(d_{p_1}, d_{p_2})n_i(d_{p_1})n_i(d_{p_2})\mathrm{d}d_{p_1}\,\mathrm{d}d_{p_2} \\ & \underbrace{-\int_0^\infty\int_0^\infty d_{p_1}^k\beta(d_{p_1}, d_{p_2})n_i(d_{p_1})n_i(d_{p_2})\mathrm{d}d_{p_1}\,\mathrm{d}d_{p_2}}_{\text{intramodal coagulation}} \\ & \underbrace{-\int_0^\infty\int_0^\infty d_{p_1}^k\beta(d_{p_1}, d_{p_2})n_i(d_{p_1})n_j(d_{p_2})\mathrm{d}d_{p_1}\,\mathrm{d}d_{p_2}}_{\text{intermodal coagulation}} \\ & + \int_0^\infty \frac{\mathrm{d}d_p^k}{\mathrm{d}v_p}\frac{\partial d_p}{\partial t}n_i(d_p)\mathrm{d}d_p + \int_0^\infty d_p^k \dot{n}_{S_i}(d_p)\mathrm{d}d_p.\end{aligned} \tag{7a}$$

MDE for Mode j

$$\frac{\partial}{\partial t}\left(M_{k_j}\right) = \nabla\cdot\mathbf{v}M_{k_j} - \nabla\cdot\int_0^\infty d_\mathrm{p}^k \mathbf{c}(d_\mathrm{p})n_j(d_\mathrm{p})\mathrm{d}d_\mathrm{p} + \nabla\cdot\int_0^\infty d_\mathrm{p}^k D(d_\mathrm{p})\nabla n_j(d_\mathrm{p})\mathrm{d}d_\mathrm{p}$$

$$+\frac{1}{2}\int_0^\infty\int_0^\infty \left(d_{\mathrm{p}_1}^3 + d_{\mathrm{p}_2}^3\right)^{k/3}\beta(d_{\mathrm{p}_1}, d_{\mathrm{p}_2})n_j(d_{\mathrm{p}_1})n_j(d_{\mathrm{p}_2})\mathrm{d}d_{\mathrm{p}_1}\,\mathrm{d}d_{\mathrm{p}_2}$$

$$\underbrace{-\int_0^\infty\int_0^\infty d_{\mathrm{p}_1}^k\,\beta(d_{\mathrm{p}_1}, d_{\mathrm{p}_2})n_j(d_{\mathrm{p}_1})n_j(d_{\mathrm{p}_2})\mathrm{d}d_{\mathrm{p}_1}\,\mathrm{d}d_{\mathrm{p}_2}}_{\text{intramodal coagulation}}$$

$$+\int_0^\infty\int_0^\infty \left(d_{\mathrm{p}_1}^3 + d_{\mathrm{p}_2}^3\right)^{k/3}\beta(d_{\mathrm{p}_1}, d_{\mathrm{p}_2})n_i(d_{\mathrm{p}_1})n_j(d_{\mathrm{p}_2})\mathrm{d}d_{\mathrm{p}_1}\,\mathrm{d}d_{\mathrm{p}_2}$$

$$\underbrace{-\int_0^\infty\int_0^\infty d_{\mathrm{p}_2}^k\,\beta(d_{\mathrm{p}_1}, d_{\mathrm{p}_2})n_i(d_{\mathrm{p}_1})n_j(d_{\mathrm{p}_2})\mathrm{d}d_{\mathrm{p}_1}\,\mathrm{d}d_{\mathrm{p}_2}}_{\text{intermodal coagulation}}$$

$$+\int_0^\infty \frac{\mathrm{d}d_\mathrm{p}^k}{\mathrm{d}v_\mathrm{p}}\frac{\partial d_\mathrm{p}}{\partial t}n_j(d_\mathrm{p})\mathrm{d}d_\mathrm{p} + \int_0^\infty d_\mathrm{p}^k \dot{n}_{S_j}(d_\mathrm{p})\mathrm{d}d_\mathrm{p}. \qquad \textbf{(7b)}$$

The *MDE for mode i* is represented by Eq. (7a) and the *MDE for mode j* is represented by Eq. (7b). The first two coagulation integrals of Eq. (7a) represent changes due to intramodal (*i-i*) coagulation, and the third coagulation integral represents a loss from mode *i* to mode *j* due to intermodal (*i-j*) coagulation. The first two coagulation integrals of Eq. (7b) represent changes due to intramodal (*j-j*) coagulation, the third coagulation integral represents gain to mode *j* due to intermodal (*i-j*) coagulation, and last coagulation integral represents loss from mode *j* due to intermodal (*i-j*) coagulation.

Choice of Moments and Mode Distribution Function. To apply Eq. (7), we must select mathematical representations for n_i and n_j and moments to evaluate. In the general formulation of the MAD model, each mode is represented by a single continuous distribution function, and the type of distribution function can be different for each mode. The choice of distribution functions is strongly motivated by mathematical convenience; selecting a distribution function that permits easy solution of the integrals in Eq. (7) reduces the subsequent computational effort. For this reason, lognormal distributions are used almost exclusively in MAD models. It turns out, however, that lognormal size distributions also provide an acceptable representation of measured aerosol distributions (e.g., see Whitby, 1978; Shimizu and Crow, 1988; and Ott, 1990). We therefore recommend use of lognormal distributions, although MAD models are not limited to lognormal distribution functions. Seo and Brock (1990) simulated evaporation in a homogeneous system, and show that a suitable representation of the particle size distribution is possible with a "double-sided" exponential function.

Lognormal distributions can be characterized by three parameters: total number concentration, N, geometric mean size of the number moment, d_{gn}, and the geometric standard deviation, σ_g. We must therefore solve differential equations for three integral moments of each lognormal distribution function used. We solve for N because it is an integral moment, but we solve for M_3 and M_6 for the following reasons. The moment M_3 is proportional to volume, and it is relatively easy to formulate terms of the MDE for processes related to volume transfer. In addition, some of the coagulation integrals for M_3 evaluate to 0.

We solve for M_6 because the term in the coagulation integral of Eq. (5)

$$\left(d_{p_1}^3 + d_{p_2}^3\right)^{k/3}$$

can be expanded to

$$d_{p_1}^6 + d_{p_1}^3 d_{p_2}^3 + d_{p_2}^6.$$

With this separation of terms and for many mathematical expressions of the coagulation coefficient (e.g., see Pratsinis, 1988 and Whitby et al., 1991), the resulting coagulation integrals of Eq. (7) can be evaluated analytically. If the integrals of Eq. (7) are evaluated numerically, then the terms in the integral do not have to be separated and any moment can be selected. Solving the integrals numerically has the advantage that a completely general model can be developed and expressions for the coefficients can be easily changed, but at increased computational effort.

THE MDE FOR A CONTINUOUS STIRRED TANK AEROSOL REACTOR

We now consider a detailed derivation of each of the terms of Eq. (7) and derive the MDE suitable for describing aerosol behavior in a continuous stirred tank aerosol reactor (CSTAR) (Pratsinis et al., 1986). In a CSTAR [represented by Fig. 2(b)] the aerosol is assumed to be homogeneously mixed in the main core of a reactor, with a boundary layer separating the homogeneous core from the wall of the reactor. Within this framework, the internal processes are only active in the homogeneous core, and the external processes only act across the boundary layer.

Internal Processes for CSTARs

Coaguation. Coagulation is viewed as a number transfer process, so the equations for the changes of moments are related to the moment change per particle collision. The model of coagulation that we use[2] is that two spherical particles collide and are subsequently lost from the system, forming, by coalescence, one new spherical particle whose volume is the sum of the volumes of the two colliding particles (we assume the sticking coefficients are unity, although this assumption can be removed). Denoting the moment lost during each collision as $(d_{p_1}^k + d_{p_2}^k)$ and the moment gained due to the appearance of the new particle as $d_{p_{12}}^k$, the net change of the integral moment is

$$\left[\frac{\partial}{\partial t}(M_k)\right]_{\text{coag}} = \frac{1}{2}\int_0^\infty \int_0^\infty d_{p_{12}}^k \beta(d_{p_1}, d_{p_2}) n(d_{p_1}) \times n(d_{p_2}) \mathrm{d}d_{p_1}\, \mathrm{d}d_{p_2} - \frac{1}{2}\int_0^\infty \int_0^\infty \left(d_{p_1}^k + d_{p_2}^k\right) \beta(d_{p_1}, d_{p_2}) \times n(d_{p_1}) n(d_{p_2}) \mathrm{d}d_{p_1}\, \mathrm{d}d_{p_2} \quad (8)$$

Note that Eq. (8) is evaluated over all sizes, without any assumptions about the mathematical form of n or β. For coagulation between spherical particles that results in the formation of a new spherical particle, the diameter of the new particle is

$$d_{p_{12}} = \left(d_{p_1}^3 + d_{p_2}^3\right)^{1/3} \quad (9)$$

By applying the modal assumption to Eq. (8), n is represented as a sum of multiple, additive distribution functions [i.e., substituting Eq. (6) into Eq. (3)]. Because Eq. (8) is an integral over two populations, we substitute $n = n_i + n_j$ and Eq. (9) into Eq. (8) to obtain

$$\left[\frac{\partial}{\partial t}(M_k)\right]_{\text{coag}} = \frac{1}{2}\int_0^\infty \int_0^\infty \left(d_{p_1}^3 + d_{p_2}^3\right)^{k/3} \beta(d_{p_1}, d_{p_2}) \times \left[n_i(d_{p_1}) + n_j(d_{p_1})\right] \times \left[n_i(d_{p_2}) + n_j(d_{p_2})\right] \mathrm{d}d_{p_1}\, \mathrm{d}d_{p_2} - \frac{1}{2}\int_0^\infty \int_0^\infty \left(d_{p_1}^k + d_{p_2}^k\right) \beta(d_{p_1}, d_{p_2})$$

[2]Reflecting our choice, rather than a limitation of MAD models.

$$\times\left[n_i(d_{p_1}) + n_j(d_{p_1})\right]$$
$$\times\left[n_i(d_{p_2}) + n_j(d_{p_2})\right]\mathrm{d}d_{p_1}\,\mathrm{d}d_{p_2}. \quad (10)$$

It is convenient to separate the terms of Eq. (10) according to the aerosol modes i and j. In order to expand and group terms, the following conventions are adopted:

- When particles from the same mode collide (intramodal coagulation), the agglomerated particle remains in that mode.
- When particles from two different modes collide (intermodal coagulation), the agglomerated particle is assigned to the mode with the larger mean size. In the derivations here, index j is used to represent the mode with the larger mean size.

The second convention is consistent with the view that the coagulating particles are growing (i.e., migrating from the smaller to the larger mode). This convention was used by Eltgroth (1982) and Whitby and Whitby (1985a and 1985b), and comparisons of the model by Whitby and Whitby (1985b) with other numerical models for bimodal coagulation (Seigneur et al., 1986) indicate that these conventions reasonably account for the migration of particles in particle size-space during coagulation.

Expanding Eq. (10) and grouping terms results in the intramodal and intermodal coagulation terms for modes i and j shown in Eq. (7). In the absence of intermodal coagulation, the intramodal terms correctly predict that V_i and V_j do not change.

The coagulation terms are completely general, and the only physical assumptions (other than the modal assumption) are unit sticking coefficients, spherical particles, and volume conservation. The intermodal coagulation terms for a distribution of three or more modes is a simple extension of the MDE for a bimodal distribution by considering the interactions between all pairs of modes.

Particle Growth. Particle growth is the process of transferring volume from the gas or vapor phases to particles. Growth processes occur by vapor condensation or by reactions on or within existing particles.

The total volume change of the particle population during growth is

$$\frac{\partial}{\partial t}(V) = \int_0^\infty \psi_p n(d_p)\mathrm{d}d_p, \quad (11)$$

where ψ_p represents the volume growth rate of size d_p particles. Because particle growth occurs by addition of gas-phase material, volume growth rates are often sensitive to thermodynamic properties. For this reason it is convenient to represent the growth rate as

$$\psi_p = \Psi_T \psi(d_p), \quad (12)$$

where Ψ_T represents the dependence of the growth rate on thermodynamic properties, and $\psi(d_p)$ represents its dependence on particle size. The general moment equation is obtained by multiplying the integrand of Eq. (11) by the specific moment change per unit volume change and substituting Eq. (12) to yield

$$\frac{\partial}{\partial t}(M_{k_i}) = \Psi_T \int_0^\infty \frac{\mathrm{d}d_p^k}{\mathrm{d}v_p}\psi(d_p)n_i(d_p)\mathrm{d}d_p. \quad (13)$$

For spherical particles the change of moment per unit change of volume is

$$\frac{\mathrm{d}d_p^k}{\mathrm{d}\left[(\pi/6)d_p^3\right]} = \frac{2k}{\pi}d_p^{k-3}. \quad (14)$$

Substituting Eq. (14) into Eq. (13) yields

$$\frac{\partial}{\partial t}(M_{k_i}) = \frac{2k}{\pi}\Psi_T \int_0^\infty d_p^{k-3}\psi(d_p)n_i(d_p)\mathrm{d}d_p. \quad (15)$$

Note that Eq. (15) correctly shows that the number moment (i.e., $k = 0$) does not change for particle growth.

Internal Sources. Internal sources may occur due to nucleation or a sudden release of particles within the system boundaries. For example, in a nuclear containment vessel, an internal explosion may create a burst of particles due to fragmentation of solid material. Nucleation of gas-phase material

would provide an additional internal source of particles. Internal sources are treated as an injection rate of particles of size d_p into the system. The injection rate of particles from all sources into mode i is

$$\frac{\partial}{\partial t}(N_i) = \sum_{S=1}^{n_s} \int_0^\infty \left[\dot{n}_S(d_p)\right]_i \mathrm{d}d_p, \qquad (16)$$

where S is the index for each source and n_s is the total number of sources. Changes of the other moments are calculated as

$$\frac{\partial}{\partial t}(M_{k_i}) = \sum_{S=1}^{n_s} \int_0^\infty d_p^k \left[\dot{n}_S(d_p)\right]_i \mathrm{d}d_p \qquad (17)$$

For multimodal distributions, algorithms must be incorporated that either direct the source aerosol into one of the existing modes or determine that a new mode should be created. To determine which of the existing modes should receive the source particles, the characteristic size of the source particles is compared with the characteristic size (e.g., d_{gn} for lognormal distribution functions) of each existing aerosol mode. If the characteristic size of the source aerosol is sufficiently different (a user-prescribed criterion) than the characteristic sizes of the existing aerosol modes, a new mode must be created. Often, however, the modes to receive source aerosol are predetermined (Whitby, 1979; Eltgroth, 1982; Giorgi, 1986; Pratsinis, 1988). Thus, resuspended dust would be included in a mode with a relatively large mean size, whereas particles resulting from vapor nucleation would be introduced into a mode with a relatively small mean size.

External Processes for CSTARs

A CSTAR is assumed to contain sufficient turbulent energy to maintain the system in a well-mixed state; this may be caused by the action of a physical stirring blade or by natural convection processes. The dynamics governing the core fluid, therefore, are the internal processes of the GDE. Near the wall, a boundary layer exists that separates the well-mixed core from conditions occurring at or near the wall. The definition of the boundary layer thickness depends on the specific process and also on particle size (Crump et al., 1983 and Fotou and Pratsinis, 1993). The processes acting across this boundary layer are considered either as inflow/outflow across the system boundaries, or as deposition to any of the internal surfaces [see Fig. 2(b)].

Inflow / Outflow. We assume that particles are small enough so that the loss from the reactor volume due to inflow/outflow processes is not size dependent. This does not imply that all of the particles in an outflow stream exit the vessel, because some might impact near the exit tube. The important point from a modeling standpoint, however, is that the aerosol sink from the CSTAR volume contains a representative sample of the entire particle size distribution.

The outflow sink term causes a loss of moment M_k at volume flow rate $Q_{R_{out}}$. An inflow source introduces moment $M_{k_{in}}$ into the vessel at volume flow rate $Q_{R_{in}}$. The expression for the net effect on M_{k_i}, due to inflows, $Q_{R_{l_{in}}}$, and outflows, $Q_{R_{l_{out}}}$, is

$$\frac{\partial}{\partial t}(M_{k_i} V_R) = \sum_{l_{in}=1}^{n_{in}} \left(M_{k_{l_{in}}}\right)_i Q_{R_{l_{in}}} - M_{k_i} \sum_{l_{out}=1}^{n_{out}} Q_{R_{l_{out}}} \qquad (18)$$

Surface Deposition. Surface losses are calculated from size-sensitive deposition velocities due to processes like gravitational settling, impaction, thermophoresis, and diffusion. The following derivation represents the combined effects of all processes reflected in the deposition velocity, ξ_S, allowing for the deposition velocity to vary for each reactor surface. The net effect on M_{k_i} is

$$\frac{\partial}{\partial t}(M_{k_i} V_R) = -\sum_{l_{su}=1}^{n_{su}} A_{l_{su}} \int_0^\infty \xi_{l_{su}}(d_p) d_p^k n_i(d_p) \mathrm{d}d_p. \qquad (19)$$

Combining the coagulation terms from Eq. (7) with Eqs. (15), (17), (18), and (19) and expanding the lhs of Eq. (19), the complete MDE for CSTARs and a bimodal aerosol can be written as

$$\frac{\partial}{\partial t}(M_{k_i}) = \sum_{l_{in}=1}^{n_{in}} \frac{(M_{k_{l_{in}}})_i Q_{R_{l_{in}}}}{V_R} - M_{k_i} \sum_{l_{out}=1}^{n_{out}} \frac{Q_{R_{l_{out}}}}{V_R} - \frac{1}{V_R} \sum_{l_{su}=1}^{n_{su}} A_{l_{su}} \int_0^\infty \xi_{l_{su}}(d_p) d_p^k n_i(d_p) \mathrm{d}d_p$$
$$+ \frac{1}{2} \int_0^\infty \int_0^\infty \left(d_{p_1}^3 + d_{p_2}^3\right)^{k/3} \beta(d_{p_1}, d_{p_2}) n_i(d_{p_1}) n_i(d_{p_2}) \mathrm{d}d_{p_1} \mathrm{d}d_{p_2}$$
$$\underbrace{- \int_0^\infty \int_0^\infty d_{p_1}^k \beta(d_{p_1}, d_{p_2}) n_i(d_{p_1}) n_i(d_{p_2}) \mathrm{d}d_{p_1} \mathrm{d}d_{p_2}}_{\text{intramodal coagulation}}$$
$$\underbrace{- \int_0^\infty \int_0^\infty d_{p_1}^k \beta(d_{p_1}, d_{p_2}) n_i(d_{p_1}) n_j(d_{p_2}) \mathrm{d}d_{p_1} \mathrm{d}d_{p_2}}_{\text{intermodal coagulation}}$$
$$+ \underbrace{\frac{2k}{\pi} \Psi_T \int_0^\infty d_p^{k-3} \psi(d_p) n_i(d_p) \mathrm{d}d_p}_{\text{growth}} + \sum_{S=1}^{n_s} \int_0^\infty d_p^k \dot{n}_{S_i}(d_p) \mathrm{d}d_p - \frac{M_{k_i}}{V_R} \frac{\mathrm{d}V_R}{\mathrm{d}t}, \qquad \textbf{(20a)}$$

$$\frac{\partial}{\partial t}(M_{k_j}) = \sum_{l_{in}=1}^{n_{in}} \frac{(M_{k_{l_{in}}})_j Q_{R_{l_{in}}}^{\text{growth}}}{V_R} - M_{k_j} \sum_{l_{out}=1}^{n_{out}} \frac{Q_{R_{l_{out}}}}{V_R} - \frac{1}{V_R} \sum_{l_{su}=1}^{n_{su}} A_{l_{su}} \int_0^\infty \xi_{l_{su}}(d_p) d_p^k n_j(d_p) \mathrm{d}d_p$$
$$+ \frac{1}{2} \int_0^\infty \int_0^\infty \left(d_{p_1}^3 + d_{p_2}^3\right)^{k/3} \beta(d_{p_1}, d_{p_2}) n_j(d_{p_1}) n_j(d_{p_2}) \mathrm{d}d_{p_1} \mathrm{d}d_{p_2}$$
$$\underbrace{- \int_0^\infty \int_0^\infty d_{p_1}^k \beta(d_{p_1}, d_{p_2}) n_j(d_{p_1}) n_j(d_{p_2}) \mathrm{d}d_{p_1} \mathrm{d}d_{p_2}}_{\text{intramodal coagulation}}$$
$$\underbrace{+ \int_0^\infty \int_0^\infty \left(d_{p_1}^3 + d_{p_2}^3\right)^{k/3} \beta(d_{p_1}, d_{p_2}) n_i(d_{p_1}) n_j(d_{p_2}) \mathrm{d}d_{p_1} \mathrm{d}d_{p_2}}_{\text{intermodal coagulation}}$$
$$\underbrace{- \int_0^\infty \int_0^\infty d_{p_2}^k \beta(d_{p_1}, d_{p_2}) n_i(d_{p_1}) n_j(d_{p_2}) \mathrm{d}d_{p_1} \mathrm{d}d_{p_2}}_{\text{intermodal coagulation}}$$
$$+ \underbrace{\frac{2k}{\pi} \Psi_T \int_0^\infty d_p^{k-3} \psi(d_p) n_j(d_p) \mathrm{d}d_p}_{\text{growth}} + \sum_{S=1}^{n_s} \int_0^\infty d_p^k \dot{n}_{S_j}(d_p) \mathrm{d}d_p - \frac{M_{k_j}}{V_R} \frac{\mathrm{d}V_R}{\mathrm{d}t}. \qquad \textbf{(20b)}$$

The last term on the rhs of Eq. (20) accounts for expansion/contraction of the vessel. Equation (20) is a volume-based MDE. For variable density systems, it is often more convenient to write the MDEs based on density. Mass-based MDEs are given by Whitby et al. (1991).

DISCUSSION

A strength of the MAD technique is that it is not necessary to specify a grid or boundary for the size domain ahead of time (as with sectional techniques); the size distribution automatically adjusts in response to the processes acting on the aerosol. Sharply peaking distributions can be easily represented, because the distribution function within each mode can contract and expand in response to the aerosol dynamics. These features of the MAD technique are particularly beneficial when simulating aerosol dynamics in chemical reactors, because the aerosol size distribution may vary over several orders of magnitude and the width of the distribution may substantially vary for simulations including particle growth and shrinkage processes. By contrast, to capture the size distribution for such a dynamic aerosol with a sectional technique, a large size range must be discretized, substantially increasing the computational effort.

A recognized problem with standard sectional techniques is numerical diffusion across section boundaries (Seigneur et al., 1986). Gelbard (1990) solved this problem for processes governed by pure volume growth by developing a moving-boundary sectional technique, but this technique is not applicable for processes including coagulation. Because there are no section boundaries within the modes of MAD models, and because the differential equations within each mode are integrated for $0 < d_p < \infty$, MAD models do not suffer from numerical diffusion and are therefore attractive for simulations including combined volume growth and coagulation. The relative ease of use and stability of considering the dynamics of a small number of modes also makes the MAD technique an attractive modeling approach.

To evaluate the accuracy and speed of aerosol modeling techniques, a comparison was made between a spline, sectional, and modal model for simulating either pure particle coagulation or volume growth (Seigneur et al., 1986). Seigneur et al. used the spline model as the standard of comparison, and evaluated the accuracy of a sectional and a modal model. Table 3 summarizes the results from the comparison. Seigneur et al. simulated the change of the aerosol size distribution for three typical atmospheric conditions: clear, hazy, and urban. The spline model was used as the standard of comparison for all cases. Table 3 shows the computational effort and average accuracy for simulations of all of the atmospheric conditions. The spline model was used as the standard of comparison, so its relative error is recorded as 0 for all cases. Because computational time is machine dependent, the time for the MAD model is shown as 1 for all simulations and the other models referenced to it. This comparison shows that for comparable accuracy, MAD models can be 100 times faster than sectional models. We note, however, that Table 3 shows results for extremely simplified cases, and the computational speed and simulation accuracy for more complex processes may vary.

Active areas of development of MAD models include algorithms for determining when modes should be added, removed, or merged with other modes; representation of multicomponent mixtures, and representation of the fractal nature of particles and

TABLE 3. Comparison of Model Results for Coagulation and Coagulation

Model	Computational Time (average relative error, percent)	
	Coagulation	Condensation
Spline	100–1000 (0%)	150 (0%)
Sectional (39 sections)	200–2000 (1%)	300 (6%)
Section (12 sections)	40–400 (2%)	100 (17%)
MAD	1 (7%)	1 (10%)

corresponding effects on the aerosol dynamics. To date no general scheme has been proposed for handling the appearance, disappearance, and merging of modes, which we broadly categorize as *dynamic mode management*. Currently, the user must preselect the number of modes to use in a simulation, and these modes persist throughout the entire calculation procedure. Youngblood and Kreidenweis (1994) used a scheme for determining when two modes should be merged based on the relative difference of condensation rates on two modes considered separately and when combined, but this technique presupposes that condensation is the dominant aerosol process. This technique may be acceptable for many types of atmospheric simulations where condensation plays an important role, but a more general approach to mode management is still needed.

Externally-mixed multicomponent aerosols can be readily represented with MAD models by using a separate mode for each chemical species. Brock and Oates (1987) used a product of two lognormal distribution functions to represent an internally mixed, two-component aerosol, but it is not clear whether this approach can be extended to a multicomponent aerosol with more than two components.

Another treatment is to apply the MAD assumption to an internally mixed multicomponent aerosol by retaining a unique mode for each possible combination of chemical components. The total number of possible combinations is

$$n_{\text{im}} = \sum_{n=1}^{n_{\text{em}}} \frac{n_{\text{em}}!}{n!(n_{\text{em}} - n)!}, \tag{21}$$

where n_{em} is the number of chemical species of an externally-mixed aerosol and n_{im} is the number of distinct chemical species for the resulting internally-mixed aerosol as. Therefore, for a three-component, externally-mixed aerosol, there are seven possible chemical components for the corresponding internally-mixed aerosol. If chemical reactions between any of the chemical species creates addition chemical compounds, then they must also be represented with additional modes. It is apparent from this discussion that for an internally-mixed, multicomponent aerosol, the number of modes can become quite large, and engineering judgment must be used to retain only those combinations that are important to the simulation. Wilck and Stratmann (1996) developed a method for representing multicomponent aerosol by using a separate log-normal size distribution to represent each independent chemical component within each mode. This is a promising technique as it extends the modal concept to represent modes within modes, and builds on the existing MAD framework. More work is needed, however, to validate the accuracy of this technique.

Another area of future work is to represent the fractal nature of particles on the aerosol dynamics. For agglomerates composed of primary particles of size r_0, Wu and Friedlander (1992) give the following relationship for the coagulation coefficient between two fractal particles

$$\beta_{12} = \left(\frac{6k_{\text{B}}T}{\rho}\right)^{1/2}\left(\frac{3}{4\pi}\right)^{\lambda} r_0^{2-6/D_{\text{f}}} \times \left(\frac{1}{v_1} + \frac{1}{v_2}\right)^{1/2} (v_1^{1/D_{\text{f}}} + v_2^{1/D_{\text{f}}})^2, \tag{22a}$$

where D_{f} is the fractal dimension $D_{\text{f}} = 3$ for a perfect sphere), r_0 is the radius of the primary particles of the fractal, and

$$\lambda = \frac{2}{D_{\text{f}}} - \frac{1}{2}. \tag{22b}$$

If constant values for D_{f} and r_0 are assumed, then Eq. (22) can be substituted into the integrals of Eq. (8) and the resulting moment integrals readily evaluated. There is not, however, a general expression for the effect of the aerosol dynamics on D_{f} and r_0, so that it is still not possible to formulate general modal equations that include the effect of fractal geometry.

SUMMARY

In this paper we showed the derivation of the governing differential equations (moment dynamic equations: MDEs) for simulating aerosol dynamics when the aerosol size distribution can be represented by multiple overlapping distribution functions. In addition, we suggested that lognormal distribution functions are a common and convenient choice for the size distribution functions of each of the component modes. The solution of the MDEs yields the moments for a set of points in time and space. With the assumption of a known form of the size distribution, the moments for each overlapping mode can be used to approximate the size distribution at any point in time or space.

Comparison with spline and sectional models show that for comparable accuracy, MAD models are up to two orders of magnitude faster. In addition, MAD models do not suffer from numerical diffusion. The speed and lack of numerical diffusion therefore make MAD models ideal for simulations involving complex physical processes where more detailed models lead to excessive numerical effort.

APPENDIX A

Relationships Between Moments and Modal Parameters of Lognormal Distribution Functions

Relationships between the modal parameters and moments of the distribution are required for MAD models. These relationships are provided here for the lognormal distribution, since this distribution is the most commonly used (for a general discussion of particle statistics and lognormal distributions, see Hinds, 1982, and Raabe, 1971). In the following expressions, subscripts k_1 and k_2 refer to specific moments (e.g., M_3 and M_6), whereas subscript k refers to an arbitrary moment. A complete description of the following expressions is provided in Appendix C of Whitby et al. (1991)

$$M_k = N d_{\mathrm{gn}}^k \exp\left(\frac{k^2}{2}\ln^2 \sigma_{\mathrm{g}}\right), \tag{A.1}$$

$$M_k = N\overline{M}_{k_1}^{\tilde{k}_1}\overline{M}_{k_2}^{\tilde{k}_2}, \tag{A.2}$$

$$d_{\mathrm{gn}} = \overline{M}_{k_1}^{\hat{k}_1}\overline{M}_{k_2}^{\hat{k}_2}, \tag{A.3}$$

$$\ln^2 \sigma_{\mathrm{g}} = \frac{2}{k_1(k_1 - k_2)}\ln\left(\overline{M}_{k_1}/\overline{M}_{k_2}^r\right), \tag{A.4}$$

where

$$\overline{M}_k = M_k/N,$$

$$r = k_1/k_2,$$

$$\tilde{k}_1 = \left[r(k/k_1)^2 - (k/k_1)\right]/(r-1),$$

$$\tilde{k}_2 = \left[r(k/k_2) - (k/k_2)^2\right]/(r-1),$$

$$\hat{k}_1 = 1/[r(k_2 - k_1)],$$

$$\hat{k}_2 = r/(k_1 - k_2).$$

References

Brock, J. R., and Oates, J. (1987). Moment Simulation of Aerosol Evaporation, *J. Aerosol. Sci.* 18(1):59–64.

Crump, J. G., Flagan, R. C., and Seinfeld, J. H. (1983). Particle Wall Loss Rates in Vessels, *Aerosol Sci. Technol.* 2(3):303–309.

Eltgroth, M. W. (1982). User's Manual for the Multiple Atmospheric General Impact Calculation Model (MAGIC), Radian Corp. Report #DCN 82-241-378-22. Austin. Texas.

Fotou, G. P., and Pratsinis, S. E. (1993). A Correlation for Particle Wall Losses by Diffusion in Dilution Chambers, *Aerosol. Sci. Technol.* 18(2):213–218.

Friedlander, S. K. (1977). *Smoke, Dust and Haze*, John Wiley and Sons, New York.

Friedlander, S. K. (1983). Dynamics of Aerosol Formation by Chemical Reaction, *Annals New York Acad. Sci.* 404:354–364.

Gelbard, F. (1990). Modeling Multicomponent Aerosol Particle Growth by Vapor Condensation, *Aerosol Sci. Technol.* 12:399–412.

Gelbard, F., and Seinfeld, J. H. (1978). Numerical Solution of the Dynamic Equation for Particulate Systems, *J. Comp. Physics* 28:357–375.

Gelbard, F., and Seinfeld, J. H. (1980). Simulation of Multicomponent Aerosol Dynamics, *J. Colloid Interface Sci.* 78(2):485–501.

Giorgi, F. (1986). Development of an Atmospheric Model for Studies of Global Budgets and Effects of Airborne Particulate Material, Ph.D. Thesis, Cooperative Thesis No. 102, Georgia Institute of Technology, Atlanta, Georgia, and National Center for Atmospheric Research, Boulder, CO.

Hinds, W. C. (1982). *Aerosol Technology*, John Wiley and Sons, New York.

Kodas, T. T., Pratsinis, S. E., and Friedlander, S. K. (1986). Aerosol Formation and Growth in a Laminar Core Reactor, *J. Colloid Interface Sci.* 111:102–111.

Lee, K. W. (1983). Change of Particle Size Distribution During Brownian Coagulation, *J. Colloid Interface Sci.* 92(2):315–325.

Lee, K. W., Curtis, L. A., and Chen, H. (1990). An Analytical Solution to Free Molecule Aerosol Coagulation. *Aerosol Sci. Technol.* 12(2):457–462.

Middleton, P., and Brock, J. (1976). Simulation of Aerosol Kinetics, *J. Colloid Interface Sci.* 54:249–264.

Ott, R. O. (1990). A Physical Explanation of the Lognormality of Pollutant Concentrations, *J. Air Waste Manage. Assoc.* 40:1378–1383.

Pratsinis, S. E., Friedlander, S. K., and Pearlstein, A. J. (1986). Aerosol Reactor Theory: Stability and Dynamics of a Continuous Stirred Tank Aerosol Reactor, *AIChE J.* 32(2):177–185.

Pratsinis, S. E. (1988). Simultaneous Aerosol, Nucleation, Condensation and Coagulation in Aerosol Reactors, *J. Colloid Interface Sci.* 124:416–417.

Raabe, O. G. (1971). Particle Size Analysis Utilizing Grouped Data and the Log-normal Distribution, *J. Aerosol Sci.* 2:289–303.

Seigneur, C., Hudischewskyj, A. B., Seinfeld, J. H., Whitby, K. T., Whitby, E. R., Brock, J. R., and Barnes, H. M. (1986). Simulation of Aerosol Dynamics: A Comparative Review of Mathematical Models, *Aerosol Sci. Technol.* 5:205–222.

Seo, Y. and Brock, J. R. (1990). Distributions for Moment Simulation of Aerosol Evaporation, *J. Aerosol Sci.* 21:511–514.

Shimizu, K., and Crow, E. L. (1988). *Lognormal Distributions*, Marcel Dekker, Inc., New York.

Whitby, K. T. (1978). The Physical Characteristics of Sulfur Aerosols, *Atmos. Environ.*, 12:135–159.

Whitby, K. T. (1979). Lumped Model Aerosol Growth Model. Particle Technology Laboratory Publication #395, Mechanical Engineering Department, University of Minnesota, Minneapolis, Minnesota.

Whitby, E. R., McMurry, P. H., Binkowski, F., and Shankar, U. (1991). Modal Aerosol Dynamics Modeling. EPA report for contract No. 68-01-7365.

Whitby, E. R., and Hoshino, M. (1996). Particle Size Distributions in a Low-pressure SiH_4:O_2:He CVD Reactor: Experimental and Numerical Results, *J. Electrochem. Soc.* 143(10), 3397–3404.

Whitby, E. R., and Whitby, K. T. (1985a). The Modal Aerosol Dynamics Model. Part 1: Solution of the Internal Terms for the General Dynamics Equation of Aerosols, U.S. EPA report for work order 5D2413NASA. Also Particle Technology Laboratory Publication #580, Department of Mechanical Engineering, University of Minnesota, Minneapolis, Minnesota.

Whitby, E. R., and Whitby, K. T. (1985b). AGROI: A FORTRAN Implementation of the Modal Aerosol Dynamics Model for the IBM PC/XT/AT. U.S. EPA report for work order 5D2413NASA. Also Particle Technology Laboratory Publication #581, Department of Mechanical Engineering, University of Minnesota, Minneapolis, Minnesota.

Wilck, M., and Stratmann, F. (1996). A Lognormal Model for the Size-resolved Treatment of Particle Dynamics and Liquid-phase Chemistry, *J. Aerosol Sci.* 27(S1), 583–584.

Williams, M. M. R. and S. K. Loyalka (1991). *Aerosol Science: Theory and Practice*, Pergamon Press.

Wu, M. K. and Friedlander, S. K. (1992). Enhanced Power Law Agglomerate Growth in the Free Molecule Regime, *J. Aerosol Sci.* 24(3):273–282.

Youngblood, D. A. and Kreidenweis, S. M. (1994). Further Development and Testing of a Bimodal Aerosol Dynamics Model, Paper #550, Colorado State Univ., Dept. of Atm. Sci.

Received March 25, 1996; accepted June 2, 1997.